Mapping the light intensity transmitted through nanoscale apertures

C500 Report

By: Nathan D. Rawlinson

Advisor: Dr. Stephen Jacobson

Introduction:

In recent years there has been much focus on the optical near field and its interesting and unique properties. The near field designates the region directly above the surface of an object (roughly half of a wavelength) and is characterized by an evanescent field (instead propagating photons) in which the intensity decays off exponentially from the surface. This characteristic of the near field of being surface bound has lead to many advances in photonics [1], plasmonics [2], sensing [3], and spectroscopy of surface species [4] (surface-enhanced Raman spectroscopy, surface plasmon resonance).

Even with many advances and uses, relatively little is known about the spatial distribution of the near field. The near field scanning optical microscope (NSOM) has been implemented to make measurements of the near field and its intensity distribution [5, 6]. With instruments such as NSOM, the instrument response is a challenge for interpreting the experimental results. Moreover, proximity NSOM probes are hard to control in their near field optical properties. Here we introduce a new way to directly determine the distribution of the transmitted light through nanoapertures without using a physical probe.

Nanoapertures have stirred an intense interest after Ebbesen's discovery of enhanced transmission through an array of sub wavelength apertures [7-9]. More recently Kwak et al. have shown that nanoapertures with diameters smaller than the incident wavelength of light generate intense electrical field gradients capable of overcoming Brownian forces and trapping small particles in a liquid with a fraction of the laser intensity required for classical optical tweezers [10,11].

In this investigation we fabricated randomly dispersed nanoapertures in a metal film by nanosphere lithography and irradiated them by UV light. The field distribution at the output of the apertures was mapped into a chemically amplified negative tone photoresist. By tuning the exposure time of the light, different intensity contours have been mapped into three dimensional polymeric nanostructures. The structures were then covered with a thin layer of gold and studied in a scanning electron microscope (SEM). It would be possible in the future to provide experimental measurements of the near field with the aid of these nanostructures and without the need of physical probes.

Experimental Section:

Nanosphere lithography (NSL) was used to synthesize randomly dispersed nanometer scale apertures in a metal film. Corning glass coverslips (No. 1, 24 x 30 mm) were prepared by cleaning them in aqua regia (3:1 stock solutions of HCl and HNO_3 respectively) for 1 hour at room temperature. The coverslips were then rinsed in water (18 MΩ·cm, Millipore Super-Q) followed by acetone and subsequently sonicated (Branson 200 Ultrasonic cleaner) for 15 min in a 3:1 solution of acetone and methanol. After sonicating, the coverslips were rinsed with acetone and dried in a stream of nitrogen. In order to promote the adsorption of the microspheres the coverslips were hydrolyzed in a solution of 0.01 M NaOH for 20 min, followed by a water rinse and sonication in water for 5 min to help remove excess salts that remain on the surface. The coverslips were then rinsed with water and dried in a nitrogen stream. Various diameters of polystyrene microspheres (114, 202, 356, 477, and 771 nm, PolyScience Inc.) were placed on the coverslips by adding 200 μl of a solution of the suspended microspheres that had been diluted to 10^{-4}% (w/v) polystyrene in water. Afterwards, the samples were

dried in low vacuum (1 torr) leaving the microspheres adsorbed to the surface of the coverslips.

In the next step the samples were coated with ~10 nm of a chromium adhesion layer followed by aluminum using thermal evaporation (CVE-20 filament evaporator). The thicknesses of the layers were monitored using a quartz microbalance (STM-100/MF, Sycon instruments). In order to achieve well defined apertures the total thickness of the Cr and Al coating was maintained to be slightly less than the radius of the microspheres used for the given sample (Figure 1). This enables the easy removal of the microspheres via sonication in methanol for 1.5 min and drying in nitrogen.

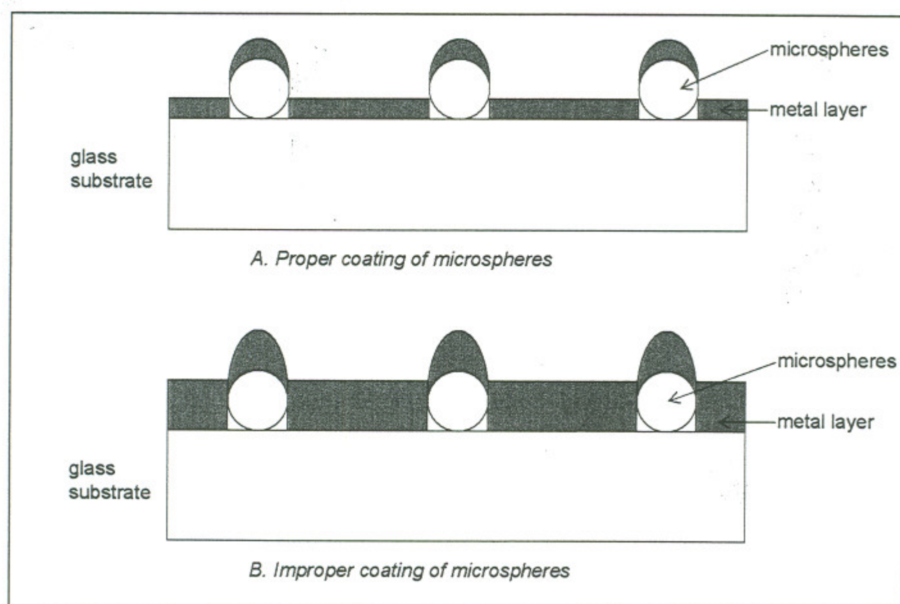

Figure 1: Shows the proper (A) and improper (B) way of coating the microspheres during the fabrication of the apertures by nanosphere lithography so that the spheres can be easily removed.

The apertures were then coated with a thin film (10-15 μm) of the negative tone photoresist SU-8 2010 (MicroChem) by spinning at 1000 rpm for 60 seconds (P6708, Speedline Technologies). The samples were prebaked for 1 min at 60°C and 3 min at 95°C (575 Digital hotplate, VWR). After which the SU-8 was exposed using a mercury

arc lamp (Spectroline 11SC-1 OP, Spectronics Corp) for various exposure times (Figure 2). The samples were held at a fixed distance of 25.4 mm away from the lamp which had an intensity of 0.5 mW/cm^2 at 365 nm. After the exposure, the samples were post baked by ramping at ~35°C /min and holding for 5 min at 95°C and, subsequently, immersed in SU-8 developer (MicroChem) for 3 min while agitating with a slight swirling motion to promote complete developing. The samples were then washed by immersing them in isopropyl alcohol and drying under low vacuum (1 torr). The resulting features, or pillars, were then sputter coated with a ~10 nm layer of gold (E5100, Polaron instruments) and analyzed in a scanning electron microscope (1430, LEO). Micrographs were taken looking at the front, side, and top of the pillars under magnifications ranging from 1 kX to 90 kX.

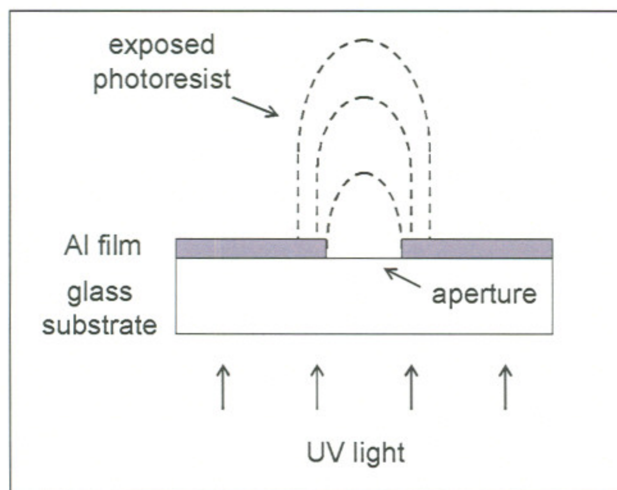

Figure 2: Schematic of experimental setup where nanometer scale apertures in a metal film on a glass substrate were used as a "mask" for photolithography. The negative tone photoresist was then exposed through the metal film mask for various exposure times which resulted in features of varying dimensions (represented by the dashed lines).

Results and Discussion:

The purpose of this investigation was to experimentally determine the light intensity transmitted through nanometer sized apertures. We varied the size of the

microspheres that were used in the fabrication of the apertures so as to span both the near-and far-field dominated regions. The diameters of the microspheres that we used to generate the apertures in this work were 114, 356, 477, and 771 nm (the 477 nm microspheres were sulfate functionalized while all other microspheres were unfunctionalized polystyrene). Figure 3 shows micrographs of the resulting pillars from this set of apertures at a constant exposure dose (3 min).

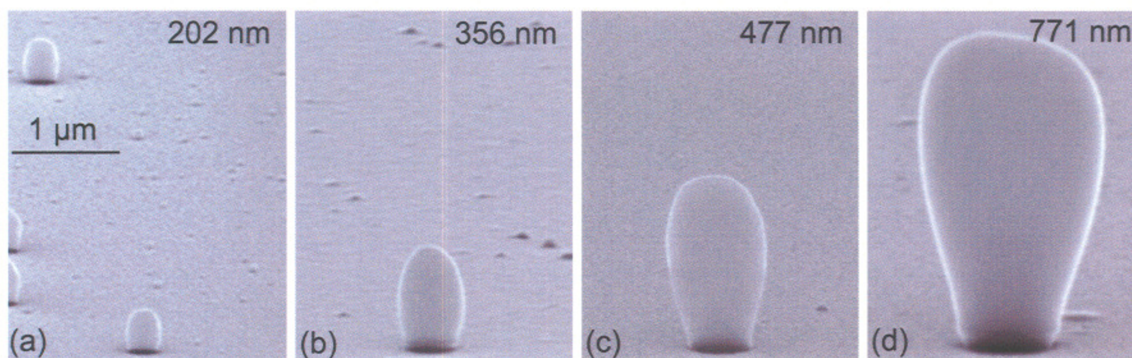

Figure 3: Comparison of the pillars resulting from varying the aperture size from the near field (a) & (b) to the far field dominated regimes (c) & (d). The shown features were exposed to the same dose of UV light from our exposure setup. All micrographs were taken at 19.2 kX magnification, 81° tilt angle, tilt corrected, and with dynamic focus enabled.

The exposures through the 114 nm apertures did not result in measurable pillars. This was due to the metal film being too thin to give good attenuation of the incident light. We found that it was difficult to get selective polymerization through the apertures when the metal film was composed of 7 nm of Cr and 40 nm of Al, which was the thickest film possible with nanosphere lithography for 114 nm apertures. There seemed to be evidence of polymerization throughout the bulk of the SU-8 photoresist. Therefore, it was very difficult to identify the polymerization emanating from the apertures. For all other apertures, the penetration of the transmitted intensity into the photoresist layer increases with aperture size (Figure 4b). The general shape of the pillars differs with

aperture size whereby the pillars generated from the smaller apertures (Figure 3a,b) were more cylindrical than pillars created using the larger apertures (Figure 3c,d).

We also probed the effect of the exposure time on the pillar size. We considered exposure times of 1, 3, 10, and 30 min. By varying the exposure time we were able to replicate the isointensity surfaces of the transmitted light through the aperture. The photoresist SU-8 has a well defined energy density threshold (mJ/cm^2) for polymerization, which is demonstrated by the ability to produce extremely straight sidewalls in conventional photolithographic processes [12]. This energy density threshold is dependent on resist processing conditions (i.e., prebake, exposure, post exposure bake, and development) and the types of features made (i.e., pillars exposed through nanoapertures versus large microfluidic channels where polymerization is needed to span the whole SU-8 film). By keeping the resist processing conditions constant, the energy density threshold was constant and the outer most surface of the pillars characterized the spatial distribution of the threshold. The exposure time needed to reach a given height is inversely proportional to the irradiance (mW/cm^2) received by the polymer at that height. The irradiance is also proportional to the square of the electric field which characterizes the isointensity surfaces. Therefore, by increasing the exposure time we mold electric field isosurfaces characterized by smaller intensities. We can then observe the trends in the dimensions of the pillars (Figure 4a) and correlate them to similar trends in isointensity surfaces.

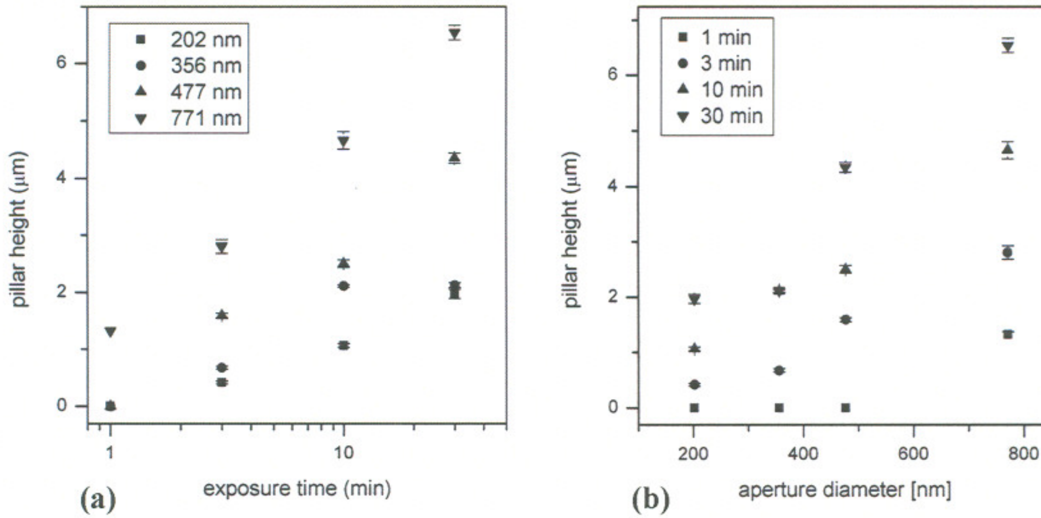

Figure 4: Variation of the pillar heights with (a) exposure time and (b) aperture diameter. The error bars are ±σ for at least 20 pillars.

If we considered the apertures as a point source and considered far field approximations, the pillar height is proportional to $t^{1/2}$ and d, where t is exposure time and d is aperture diameter (Equation 2).

$$\Phi_{th} = \frac{T \cdot I_o \cdot t}{z^2} \qquad \text{Equation 1}$$

Equation 1 rearranged for z yields

$$z = \sqrt{\frac{T \cdot I_o \cdot t}{\Phi_{th}}} \qquad \text{Equation 2}$$

where Φ_{th} is energy density threshold of the SU-8, I_o is radiant power of the lamp, T is transmittance (which is proportional to d), and z is the height of the pillar. Therefore, the change in pillar height with time and aperture diameter would both show up as linear trends on the graphs in Figure 4 (log of exposure time). We observed that the larger diameter apertures show good linearity (R=0.999, 0.990 for 771 and 477 nm

respectively), while the smaller apertures have a slight deviation from linearity (R=0.952, 0.986 for 356 and 202 nm respectively). The quality of the fit for the 356 nm apertures is low, and can be explained by the fact that the 30 min exposure is not consistent with the rest of the data and therefore appears to be an anomaly. We can therefore see that the larger aperture sizes and longer exposure times behave like the far field with respect to the height of the pillars whereas the smaller sizes and shorter times may have other influences that cause this deviation from linearity. Yet, if the apertures were strictly behaving as a far field emitter, they would tend to emit as a dipole. The shape of our pillars is not exactly what would be expected from a far field emitter, and the influences of the near field could be contributing to this difference in shape.

The 1 min exposures had evidence of polymerization in and around the apertures but standing pillars were only achieved for the 771 nm apertures at that exposure time. Further resist processing would be required in order to achieve standing pillars for the other aperture diameters at 1 min exposure. The 1 min exposures that did not result in standing features (202, 356, 477 nm apertures) were considered as a height of 0 nm.

From the data presented in Figure 4, we believe this near-field photolithographic technique can be used for fabricating nanoscale features of varying dimensions. This can be accomplished simply by tuning the exposure time and aperture diameter. Figure 5 shows the data from Figure 4 projected into the aperture diameter and exposure time plane. Superimposed on the plot is a contour plot generated by linear interpolation of the data in Figure 4. Such plots can be used to guide the experimental conditions needed to fabricate nanoscale features of desired dimensions for various applications [13].

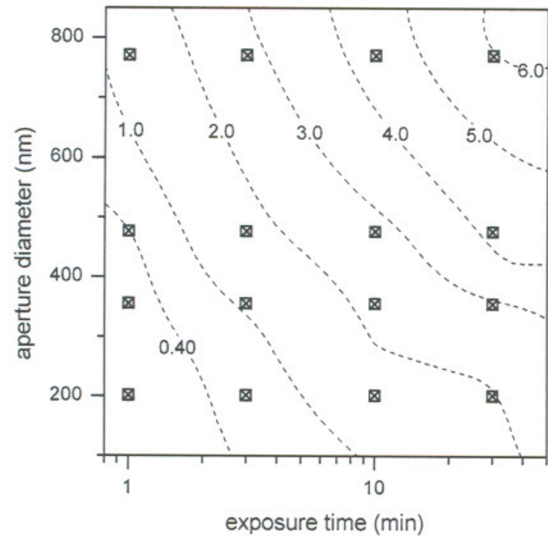

Figure 5: Contour plot of the linearly interpolated data from Figure 4. The contours are in units of microns, and the symbols represent the data from Figure 4.

Another interesting result that we found was the effect of polarized light on the shape of the pillars. For the exposure step of the pillar fabrication, we used partially polarized light ($I_x/I_y = 1.5$). The polarized light created asymmetric pillars whose face parallel to the direction of polarization is wider than the side orthogonal to the polarization (Figure 6).

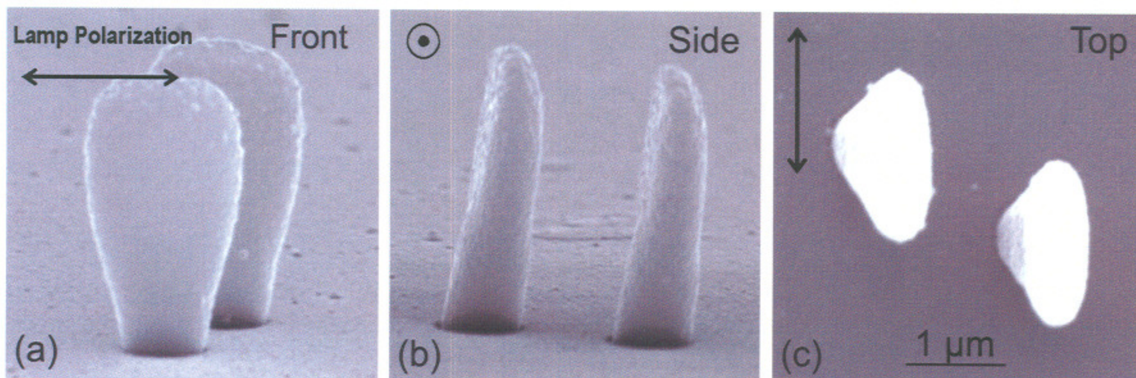

Figure 6: SEM micrographs of the same two asymmetric pillars (771 nm aperture, 3 min exposure) shown from the front, side and top. All three micrographs were taken at 13.5 kX magnification, and figures (a) & (b) were taken at 81° tilt angle, tilt corrected, and with dynamic focus on.

We measured the aspect ratio of these asymmetric pillars (width at half-height of the face in the plane of polarization/side orthogonal to the polarization), and we found that this effect of asymmetric polymerization was more pronounced as the aperture diameter was increased (Figure 7). The aspect ratio was only dependent on the aperture diameter, and was constant with the exposure time within experimental error. We explain this fact by considering that the light coming from places on the aperture wall where the incident light is *s*-polarized is more strongly attenuated in far field whereas *p*-polarized light suffers less attenuation (Figure 8). In the region close to the surface of the aperture, where the near field dominates, the difference in attenuation of *s*- and *p*-polarized light due to scattering of photons is not so evident because the near field contributes a local evanescent field at the surface of the metal. Yet, this evanescent field dies off quickly so that as the pillar height is increased there is less evanescent contribution and the difference in attenuation of the *s*- and *p*-polarized light will be more prevalent. This phenomenon can be seen at the base of the structures developed in the far field where we notice that the base presents cylindrical symmetry. This may be due to the transmitted light close to the metal surface having more contribution from the near field than the region at half-height.

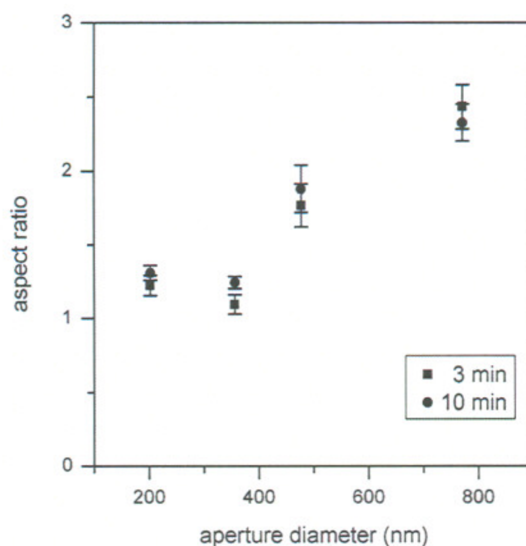

Figure 7: Variation of the aspect ratio (width measured at half-height of front/side) of the asymmetric pillars with aperture diameter. For the 3 and 10 min exposure the aspect ratio is constant within experimental error with exposure time.

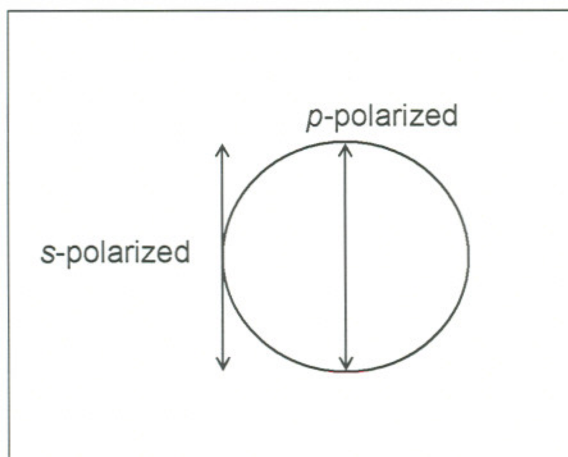

Figure 8: Schematic of the top view of an aperture. Shows how incident light with a given polarization can be considered as both s- and p-polarized with respect to the wall of the aperture.

Conclusions:

We have successfully developed a new method for directly looking at the spatial distribution of light transmitted through nanometer scale apertures. Furthermore, because this method is an inexpensive and tunable way to generate nanometer scale features of a

nonconducting material, we believe that several fields including nanoimprinting [14], photonics, and sensing may adopt such techniques.

Presently, we are limited by nanosphere lithography to produce apertures with smaller diameters and sufficient light attenuation by the metal film. Therefore. we plan to begin using electron beam lithography to generate smaller apertures (e.g., 50-100 nm). We would then be able to probe even further into the regime dominated by the near field. Electron beam lithography also has the ability to produce ordered arrays of apertures. This method would provide a way of looking directly at the transmitted light using 3 dimensional polymeric nanostructures. Ordered arrays of nanostructures may have interesting spectroscopic properties that could be used in sensing and light amplification. The effects of polarized light can also be used to generate different sets of asymmetric features through the same array of apertures simply by changing the direction of polarization.

Acknowledgements:

N.D.R. would like to thank Professor Bogdan Dragnea and Dragos Amarie for their help on this project.

References:

[1] Hillenbrand, R., *Ultramicroscopy,* **2004,** 100, 421-427 AUG 2004

[2] Maier, S.; Brongersma, M.; Kik, P.; Meltzer, S.; Requicha, A.; Atwater, H., *Adv Mater*, **2001**, 13, 1501-1505

[3] Lechuga, L.; Calle, A.; Prieto, F., *Quim Anal,* **2000**, 19, 54-60

[4] Micic, M.; Klymyshyn, N.; Lu, H., *J Phys Chem B*, **2004**, 108, 2939-2947

[5] Betzig, E.; Trautman, J., *Science* **1992,** 257, 189

[6] Zenhausern, F.; O'Boyle, M.; Wickramasinghe, K., *Appl. Phys. Lett.* **1994,** 65, 1623-1625

[7] Ebbesen, T.W.; Lezec, H.J.; Ghaemi, H.F.; Thio, T.; Wolff, P.A., *Nature* **1998,** 391, 667-669

[8] Ghaemi, H.F.; Thio, T.; Grupp, D.E.; Ebbesen, T.W.; Lezec, H.J., *Phys. Rev. B* **1998**, 58, 6779-6782

[9] Kim, T.J.; Thio, T.; Ebbesen, T.W.; Grupp, D.E.; Lezec, H.J., *Opt. Lett.* **1999,** 24, 256-258

[10] Kwak, E.S.; Onuta, T.D.; Amarie, D.; Portyrailo, R.; Stein, B.; Jacobson, S.; Schaich, W.L.; Dragnea, *J. Phys. Chem. B* **2004,** in press

[11] Ashkin, A., *Phys. Rev. Lett.* **1970**, 24, 156-159

[12] Dentinger, P.; Krafcik, K.; Simison, K.; Janek, R.; Hachman, J., *Microelectron Eng.* **2002,** 61-62, 1001-1007

[13] Kim, H.; Wallraff, G.; Kreller, C.; Angelos, S.; Lee, V.; Volksen, W.; Miller, R.D., *Nano Lett.* **2004,** ASAP, nl0498738

[14] Guo, L.J., *J Phys D: Appl Phys,* **2004**, 37, R123-R141